Analyzing the encoding range of amplitude-phase coupled spatial light modulators

Robert W. Cohn, MEMBER SPIE
University of Louisville
The ElectroOptics Research Institute
Louisville, Kentucky 40292
E-mail: rwcohn01@ulkyvm.louisville.edu

Abstract. Most spatial light modulators (SLMs) are limited in that they cannot produce arbitrary complex modulations. Because phase and amplitude are usually coupled, it is difficult to computer design appropriate modulation patterns fast enough for the real-time applications for which SLMs are suited. Dramatic computational speedups can be achieved by using encoding algorithms that directly translate desired complex values into values that the modulator can produce. For coherently illuminated SLMs in a Fourier transform arrangement, pseudorandom encoding can be used. Each SLM pixel is programmed in sequence by selecting a single value of pixel modulation from a random distribution having an average that is identical to the desired fully complex modulation. While the method approximates fairly arbitrary complex modulations, there are always some complex values that are outside the encoding range for each SLM coupling characteristic and for each specific pseudorandom algorithm. Using the binary random distribution leads to methods of evaluating and geometrically interpreting the encoding range. Evaluations are presented of achieving fully complex encoding with SLMs that produce less than 2π of phase shift, identifying an infinite set of encoding algorithms that encode the same value, identification of the maximum encoding range, and geometric interpretation of encoding errors. [S0091-3286(99)01702-X]

Subject terms: spatial light modulators; computer generated holography; complex-valued encoding; statistical optics.

Paper 980184 received May 5, 1998; revised manuscript received Sep. 14, 1998; accepted for publication Sep. 24, 1998. This paper is a revision of a paper presented at the SPIE Conference on Spatial Light Modulators, January 29–30, 1998, San Jose, CA. The paper presented there appears (unrefereed) in Proc. SPIE Vol. 3297 (1998).

1 Introduction

The encoding of fully complex functions onto computer generated Fourier transform holograms was first introduced by Brown and Lohmann.[1,2] The method and other subsequent fully complex encoding methods, reviewed in Refs. 3 to 5, provide the ability to transparently specify desired far-field diffraction patterns in terms of Fourier transform identities, tables and other well known relationships, many that are known in closed form. An example of a system application is the potential of using phase-only spatial light modulators (SLMs) to produce and steer multiple spots in arbitrary directions independent of each other in real time.[6] The ability to directly encode and represent desired complex valued modulation provides the numerical efficiency required to design a continuous stream of modulations in real time. Other real-time applications that can benefit from complex-valued representations are considered in Ref. 5. Additional advantages of complex valued representations in terms of the fidelity of computer generated holograms (CGHs) and diffractive optical elements were also considered by Kettunen et al.[7] Certainly the recognition of these various advantages has also spurred the development and demonstration of fully complex modulators.[8–11] No fully complex SLM is commercially available, however, and the most recent demonstrations of fully complex SLMs require the use of multiple SLMs. For these reasons, complex-valued representations continue to be of interest.

Most of the early CGH design methods treat multiple pixels as a single group to realize a single complex value. By grouping pixels, the space-bandwidth product of the signal is necessarily less than that of the CGH. Therefore the useable bandwidth of the reconstruction is limited to only a fraction of the entire bandwidth set by the pixel sample spacing. This is especially important today when electrically addressed SLMs are relatively expensive and consist of a small number of pixels compared to fixed pattern CGHs and diffractive optics.

One early technique that does use a single pixel to represent a complex value is the original kinoform, in which the magnitudes of each complex value are set to unity.[12] Due to noise and inaccuracies in the reconstruction,[7] however, most phase-only CGHs now are designed using various numerically intensive global search algorithms.[13–18] In some real-time systems, the filter design may need to be done on-line, which may not enable global searches to be performed. Other single pixel methods are the minimum

Euclidean distance (MED) methods for matched filter[19] and CGH (Ref. 20) design. MED optimizes a performance metric as a function of a complex-valued factor that scales all the desired complex values. The performance metric is calculated for each value of the scale factor. Once the optimum scale factor is found, each desired complex value is mapped to the closest realizable value on the modulation characteristic. This two parameter search requires considerably less computation to perform than the global searches.

MED and related studies[21,22] are important in that they describe filter design methods in such ways that the methods apply to a wide variety of modulation characteristics. This recognizes the fact that current electrically and optically addressed SLMs have widely varied modulation characteristics that are usually not accurately described as being pure phase or amplitude modulators. Instead, these SLMs exhibit various degrees of coupling between amplitude and phase, as reported in a number of papers on SLM modulation characteristics.[23–26]

Pseudorandom encoding,[27] the subject of this paper, is a single pixel method that has been primarily applied to CGH design. The procedure for mapping a desired complex value to a realizable pixel modulation is a noniterative and numerically efficient operation. When the CGH is illuminated by a uniform plane wave, the far-field diffraction pattern approximates the desired reconstruction in an average sense. Superimposed on the desired reconstruction is a white noise pattern that covers the entire reconstruction plane. The energy in the noise is equivalent to the errors between the desired complex values and the realized values. By spreading the noise over the full extent of the reconstruction plane, the noise level is, on average, the lowest possible for a fixed level of error energy. This can be compared[28] with error diffusion methods for CGHs. The reconstruction from the error diffused hologram also produces a noise cloud, but the noise cloud and desired reconstruction appear in different regions of the reconstruction plane. Thus, unlike error diffusion, pseudorandom encoding enables the desired reconstruction to be formed anywhere in the full extent of the reconstruction plane. The noise level from pseudorandom encoding a particular signal still might be unacceptably high, however, there are simple calculations that can be performed prior to encoding that measure the noise,[27,29] and many pseudorandom encoded designs with negligible noise backgrounds have been reported to date.[27,29–31]

Originally pseudorandom encoding was introduced[27] for phase-only SLMs, and then ways to generalize this method to amplitude-phase coupled modulators were considered.[31] A useful result from this study was the development of a closed form encoding algorithm in which the values of any given coupled modulation characteristic could be explicitly placed in the formula.[31] However, numerical evaluations show that some complex values could not be encoded by this method. These observations led to more fundamental analyses of the properties of pseudorandom encoding, including the encoding range and the amount of error signal produced by encoding. The greatest progress was made by using binary statistics that, in addition to numerical ease, provide useful geometrical interpretations of various properties of the pseudorandom encoding methods. This paper specifically describes this analysis technique and presents examples that, in addition to illustrating the analysis technique, are used to identify properties of pseudorandom encoding that were not previously known. Sec. 2 reviews the mathematics of pseudorandom encoding and specializes the problem for the use of binary statistics. Then in Sec. 3, these tools are applied to evaluating the encoding range and encoding errors for SLMs having a variety of modulation characteristics.

2 Pseudorandom Encoding of Fully Complex Functions

2.1 *General Description of Pseudorandom Encoding*

All pseudorandom encoding algorithms specify the modulation of any given pixel in terms of a user specified random variable. The statistical properties of the random variable are selected in such a way that the expected value, or average, of the random modulation is identical to the desired, but unobtainable, fully complex value. The desired complex-valued modulation is written $\mathbf{a}_c=(a_c,\psi_c)$ and the resulting modulation by the SLM is $\mathbf{a}=(a,\psi)$, where the ordered pairs are the polar representations of the complex quantities. Complex quantities are indicated by bold type. The pseudorandom encoding design statement is, in general, to find a value of the ensemble average

$$\langle \mathbf{a} \rangle = \int \mathbf{a} p(\mathbf{a}) \mathrm{d}\mathbf{a}, \tag{1}$$

of the random variable $\mathbf{a}$ such that $\langle \mathbf{a} \rangle = \mathbf{a}_c$. The statistical properties of $\mathbf{a}$ are determined by its probability density function $p(\mathbf{a})$. The probability density function (pdf) is *selected* to ensure that the expected value of $\mathbf{a}$ and the desired complex value are identical. This *selection* of a pdf corresponds to solving the integral equation, Eq. (1) for $p(\mathbf{a})$. The solution is not unique since the integral in Eq. (1) is a projection from the multidimensional space of $\mathbf{a}$ into a single value $\langle \mathbf{a} \rangle$. After an appropriate density function is determined, the desired complex value $\mathbf{a}_c$ is encoded by drawing a single value of $\mathbf{a}$ from a random distribution having the density function $p(\mathbf{a})$. Since the value of $\mathbf{a}$ is found deterministically by computer, rather than from a random process occurring in nature, the procedure has been termed pseudorandom encoding.

This general pseudorandom encoding prescription is applied to each pixel in sequence to encode the desired spatially varying complex modulations $\mathbf{a}_c$. Using i as the spatial coordinate, the spatial samples of the desired complex modulation, the density function and the random modulation can be written as $\mathbf{a}_{ci}$, $p_i(\mathbf{a}_i)$ and $\mathbf{a}_i$. (This indexing scheme can be conveniently applied to 1-D or 2-D arrays and it is not restricted to equally spaced samples.)

The far-field diffraction pattern of the encoded modulation $\mathbf{a}_i$ approximates the desired diffraction pattern. This can be seen by comparing the intensity of the desired far-field diffraction pattern with the ensemble average diffraction pattern that would result from the encoded modulation. The intensity pattern of the desired diffraction pattern from an N sample fully complex SLM is

$$I_c(f_x)=\left|\sum_{i=1}^{N}\mathbf{A}_{ci}\right|^2=\left|\mathcal{F}\left(\sum_{i=1}^{N}\mathbf{a}_{ci}\right)\right|^2, \tag{2}$$

where $\mathcal{F}\{\cdot\}$ is the Fourier transform operator, $\mathbf{A}_{ci}(f_x)$ is the Fourier transform of the transmittance of the i'th pixel of the SLM, and f_x is the spatial coordinate across the Fourier plane. The expected intensity of the diffraction pattern from the encoded modulation was derived for the condition that the random variable $\mathbf{a}_i$ for the i'th pixel is statistically independent of $\mathbf{a}_j$ for all j not equal to i. Under the pseudorandom design condition $\langle\mathbf{a}_i\rangle=\mathbf{a}_{ci}$ the ensemble average pattern is expressed[27,29]

$$\langle I(f_x)\rangle=I_c(f_x)+\sum_{i=1}^{N}(\langle|\mathbf{A}_i|^2\rangle-|\mathbf{A}_{ci}|^2), \tag{3}$$

where $\mathbf{A}_i(f_x)$ is the Fourier transform of $\mathbf{a}_i$. The expected intensity consists of two terms. The first term is the desired diffraction pattern from Eq. (2). The second term, the N term summation, represents the average level of background (i.e., speckle) noise that is produced as a result of the randomness of the modulation. It is the error signal referred to in the introduction. For the case of pixels that are modeled as pointlike apertures, the average background noise is of constant intensity for all frequencies f_x (i.e., it is white.)

2.2 *Encoding Error Defined*

Eq. (3) identifies individually the noise contribution of each pixel. Therefore insight can be gained by evaluating the noise contribution in the modulation plane. Under the assumption that the pixels are infinitesimally wide apertures, the inverse Fourier transform of the noise from a single SLM pixel [i.e., a single term from the summation in Eq. (3)] gives the encoding error

$$\varepsilon=\langle|\mathbf{a}|^2\rangle-|\mathbf{a}_c|^2, \tag{4}$$

where the subscript has been dropped to simplify presentation. (If the pixels are finite width, then an autocorrelation of the pixel aperture function would also be included in the formula.[27] This term is dropped because it adds no essential insight to the current discussion.) In the next subsection Eqs. (1) and (4) are specialized for the case where $\mathbf{a}$ is a binary random variable.

2.3 *Pseudorandom Encoding with the Binary Distribution and Geometric Interpretation*

The probability density function for the binary distribution is

$$p(\mathbf{a})=d\,\delta(\mathbf{a}-\mathbf{a}_1)+(1-d)\,\delta(\mathbf{a}-\mathbf{a}_2), \tag{5}$$

where $\delta(\cdot)$ is the Dirac delta function, $\mathbf{a}_1$ and $\mathbf{a}_2$ are a pair of complex values from the modulation characteristic and d and $1-d$ are the probabilities of selecting $\mathbf{a}_1$ and $\mathbf{a}_2$. Since d is a probability, its value is between 1 and 0. Using the binary density function in Eq. (1) gives an expression for the effective complex amplitude of

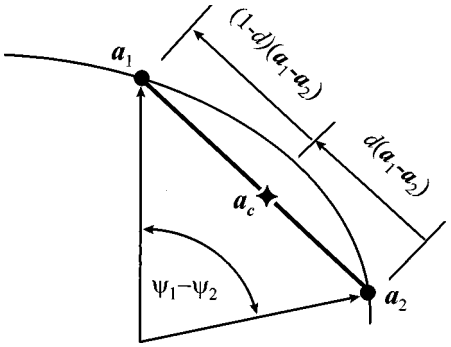

Fig. 1 Geometric relationships for pseudorandom encoding the desired value $\mathbf{a}_c$ using random binary selection of modulator values $\mathbf{a}_1$ and $\mathbf{a}_2$.

$$\langle\mathbf{a}\rangle=d\,\mathbf{a}_1+(1-d)\mathbf{a}_2. \tag{6}$$

Eq. (6) is recognized as the expression for a line as a function of the variable d. For $d=1$, $\mathbf{a}_1$ is encoded, for $d=0$, $\mathbf{a}_2$ is encoded and for values of d between 1 and 0, any value lying on the line segment between $\mathbf{a}_1$ and $\mathbf{a}_2$ can be encoded. Therefore, the *encoding range* of pseudorandom binary encoding is the line segment that connects $\mathbf{a}_1$ to $\mathbf{a}_2$ as illustrated in Fig. 1.

2.3.1 *The binary encoding formula*

For a given value of d the desired complex value $\mathbf{a}_c(d)=\langle\mathbf{a}\rangle$ is represented (i.e., encoded) by a single randomly selected value

$$\begin{aligned}&\mathbf{a}=\mathbf{a}_1 \quad \text{if} \quad 0\leqslant s\leqslant d,\\ &\mathbf{a}=\mathbf{a}_2 \quad \text{if} \quad d<s\leqslant 1,\end{aligned} \tag{7}$$

where s is a uniformly distributed random number between 0 and 1.

2.3.2 *Binary encoding error*

Evaluating Eq. (4) using Eqs. (5) and (6) and the expectation

$$\langle|\mathbf{a}|^2\rangle=d|\mathbf{a}_1|^2+(1-d)|\mathbf{a}_2|^2, \tag{8}$$

the encoding error can be written

$$\varepsilon=d(1-d)[a_1^2+a_2^2-2a_1a_2\cos(\psi_1-\psi_2)]. \tag{9}$$

The error is written in terms of the magnitudes and phases of $\mathbf{a}_i=(a_i,\psi_i)$ to show that the term in the brackets is the familiar formula for the ''law of cosines,'' which gives the squared magnitude of the line segment $\mathbf{a}_1-\mathbf{a}_2$. Thus the encoding error can be written

$$\varepsilon=d(1-d)|\mathbf{a}_1-\mathbf{a}_2|^2. \tag{10}$$

Using the main premise of pseudorandom encoding that $\mathbf{a}_c\equiv\langle\mathbf{a}\rangle$, Eq. (6) can be rearranged to make the two relationships evident

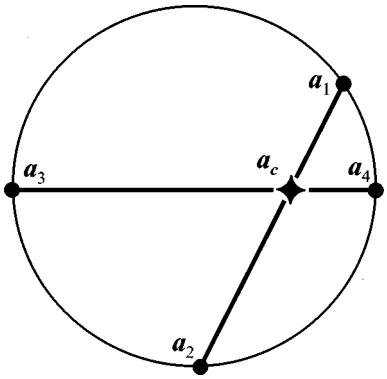

Fig. 2 Multiple possible pairs of modulation values (joined by chords) that can pseudorandom encode the desired value $\mathbf{a}_c$ for a circular modulation characteristic. This construction shows that there are an infinite number of possible binary pairs that encode $\mathbf{a}_c$.

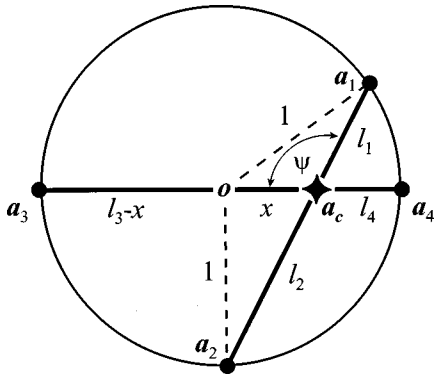

Fig. 3 Geometric relationships used to prove that for a circular modulation characteristic, the encoding error is identical for encoding with any pair of points from the modulation characteristic that are collinear with the desired value $\mathbf{a}_c$.

$$\mathbf{a}_c-\mathbf{a}_2=d(\mathbf{a}_1-\mathbf{a}_2),$$
$$\mathbf{a}_1-\mathbf{a}_c=(1-d)(\mathbf{a}_1-\mathbf{a}_2). \tag{11}$$

These lengths are indicated on Fig. 1. Using Eq. (11) in Eq. (10) shows that binary pseudorandom encoding error can be expressed as

$$\varepsilon=|\mathbf{a}_1-\mathbf{a}_c||\mathbf{a}_c-\mathbf{a}_2|. \tag{12}$$

Written in this form, the encoding error can be directly interpreted as the product of the lengths of the line segments $\mathbf{a}_1$ to $\mathbf{a}_c$ and $\mathbf{a}_c$ to $\mathbf{a}_2$.

This section has (1) identified [following Eq. (6)] that the pseudorandom encoding range for any pair of complex valued points is the line segment connecting those two points and (2) derived [Eq. (12)] that the encoding error is equal to the product of the lengths of the two line segments that connect $\mathbf{a}_1$ to $\mathbf{a}_c$ and $\mathbf{a}_2$ to $\mathbf{a}_c$. These two basic results provide a useful tool for evaluating and understanding the encoding properties of various coupled SLM characteristics and, ultimately, developing new pseudorandom encoding algorithms for specific modulation characteristics. Their application to the analysis of a variety of coupled modulation characteristics is illustrated by the examples that follow in Sec. 3.

3 Illustrative Analyses of Pseudorandom Encoding on Coupled SLMs

3.1 *Phase-Only and Circular Modulation Characteristics*

Figure 2 shows a circular modulation characteristic on the complex plane. This is more general than phase-only because the center of the modulation characteristic (or curve) is not necessarily located at zero. Off centered curves are typical of birefringent liquid crystal SLMs used with a polarizer. As the polarizer is rotated away from the extraordinary axis, the center of the modulation characteristic moves away from the origin in the complex plane. Thus this characteristic can be viewed as coupled in amplitude and phase. However, it is not necessary to write the relationship between amplitude and phase for the evaluations to be considered here.

Figure 2 illustrates two interesting properties of pseudorandom encoding for circular modulation characteristics. First, it can be seen by repeated plottings of Eq. (6) for different values of $\mathbf{a}_i$ and $\mathbf{a}_2$ that any complex value inside the circular characteristic can be encoded by choosing a pair of points from the characteristic that are colinear with the desired complex value $\mathbf{a}_c$. Second, it can be seen that since probability d of selecting one endpoint can never exceed unity, no complex values outside the characteristic can be pseudorandom encoded. Third, it can be seen that there are multiple pairs of points that can encode the same value $\mathbf{a}_c$. Obviously there are an infinite number of solutions. This nonuniqueness of pseudorandom encoding was described in general in the text following Eq. (1).

If there are multiple solutions possible, is there one particular one that produces the least encoding error? It turns out that for circular characteristics, the encoding error is identical for all possible solutions. This can be proved using the geometric constructions in Fig. 3. For this statement to be true then according to Eq. (12)

$$\varepsilon_c=l_1l_2=l_3l_4, \tag{13}$$

where l_i are the distances from the points $\mathbf{a}_i$ to $\mathbf{a}_c$. The line segment $\mathbf{a}_1$ to $\mathbf{a}_2$ in Fig. 3 passes through the center of the circle. The radius of the circle can be assumed to be unity with no loss in generality. Also defining $x=1-l_3$ as the distance from the center to $\mathbf{a}_c$ leads to a straightforward derivation. The law of cosines gives the expressions

$$l_1^2-2xl_1\cos\psi-(1-x^2)=0,$$
$$l_2^2+2xl_2\cos\psi-(1-x^2)=0, \tag{14}$$

where $-\cos\psi=\cos(\pi-\psi)$ has been used to eliminate the complementary angle $\pi-\psi$ from the second expression in Eq. (14). The positive roots to the quadratic equations are

$$l_1=x\cos\psi+(x^2\cos^2\psi+1-x^2)^{1/2},$$

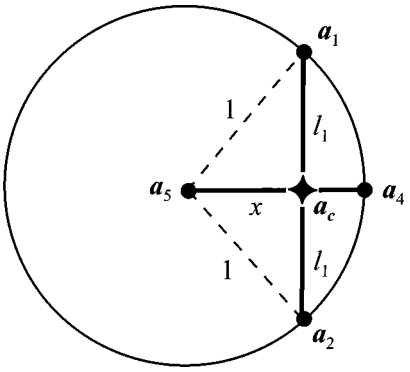

Fig. 4 Constructions used in the comparison of the encoding error for biradial and circular modulation characteristics. We show in the text that when encoding the desired value $\mathbf{a}_c$, the error is always lower if the biradial modulation values $\mathbf{a}_4$ and $\mathbf{a}_5$ are used rather than the values $\mathbf{a}_1$ and $\mathbf{a}_2$ from the single radius portion of the modulation characteristic.

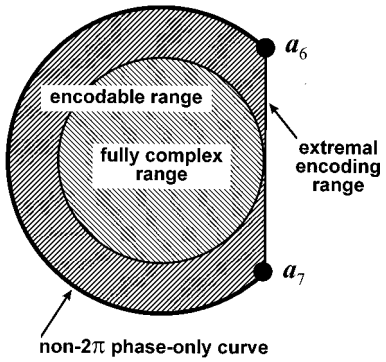

Fig. 5 Encoding range (shaded) for a non-2π phase-only SLM (thick curve). The thin line represents the values that can be pseudorandom encoded using the endpoints $\mathbf{a}_6$ and $\mathbf{a}_7$ of the modulation characteristic. The fully complex range is the largest circular region surrounding the origin. Therefore the non-2π modulator can represent a fully complex modulator if the desired complex-valued modulation are scaled so that their values fit within the fully complex region.

$$l_2 = -x\cos\psi + (x^2\cos^2\psi + 1 - x^2)^{1/2}. \tag{15}$$

The product of the two lengths then simplifies to

$$\varepsilon_c = l_1 l_2 = (1+x)(1-x), \tag{16}$$

which is independent of angle ψ and which is seen by inspection of Fig. 3 to be identical to $l_3 l_4$.

3.2 *Biradial Circular Modulation Characteristics*

Figure 4 shows a circular SLM characteristic that, in addition to the Fig. 2 characteristic, also can produce a modulation state at the center of the circle. For characteristics centered on the origin, this would be a phase-only SLM that also contains a 0 state. Using the geometric construction in Fig. 4, we can see that the encoding error produced by encoding with the points $\mathbf{a}_5$ and $\mathbf{a}_4$ is

$$\varepsilon_b = l_5 l_4 = x(1-x). \tag{17}$$

From the result in Eq. (16) or from the geometry in Fig. 4 we can see that encoding with the central point always produces less error than does biamplitude encoding with a phase-only SLM. For a unit radius circular characteristic $x = d$ and the ratio of the two types of error reduces to

$$\frac{\varepsilon_c}{\varepsilon_b} = 1 + \frac{1}{d}. \tag{18}$$

Thus the encoding errors are always lower for the biradial SLM and substantially better when the desired complex values are close to zero.

3.3 *Non-2π SLMs, Discrete SLMs and Convoluted Modulation Characteristics*

Figure 5 shows a phase-only SLM that does not produce a full 2π of phase modulation. The curve starts with point $\mathbf{a}_6$ and ends with point $\mathbf{a}_7$. Obviously, any value on a line between these two points can be pseudorandom encoded. Also line segments can be drawn that fill in the interior of the region bounded by the modulation curve and the extremal line segment $\mathbf{a}_6$ to $\mathbf{a}_7$. The interior region (shown by both shading patterns) forms a convex set. The key result of this analysis is that by appropriately scaling the desired complex values (to fit within the circular, fully complex region in Fig. 5) it would be possible to pseudorandom encode any fully complex function with the non-2π phase-only characteristic.

Figure 6 shows a convoluted characteristic. Some complex values that in a sense are *outside* the modulation characteristic can also be encoded by binary pseudorandom encoding. There are three extremal line segments in Fig. 6 that, together with the convex portions of the modulation curve, define the boundary on the convex set of encodable values. Using binary encoding analysis to evaluate the encoding range shows that the encoding range can be significantly larger than one might at first assume.

The encoding range of a discrete modulation characteristic is evaluated in Fig. 7. Here only values on the six line

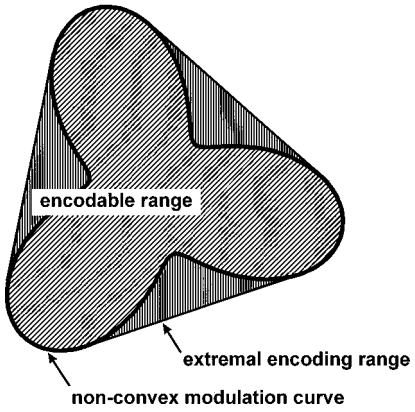

Fig. 6 Encoding range for a nonconvex modulation characteristic (thick curve). The three thin lines together with the convex portions of the SLM bound the convex region that can be pseudorandom encoded. The two shading patterns are used to distinguish the nonconvex region inside the modulation characteristic from the additional range that the analysis using the properties of binary statistics has identified as being encodable.

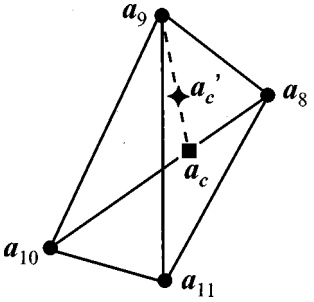

Fig. 7 Encoding range for a four-value discrete modulation characteristic. Binary pseudorandom encoding only encodes values on the six line segments. However, any other value (e.g., $\mathbf{a}_c'$) in the convex region bounded by the lines connecting $\mathbf{a}_8$, $\mathbf{a}_9$, $\mathbf{a}_{10}$, $\mathbf{a}_{11}$, and $\mathbf{a}_8$ could be encoded by a combination of binary encoding algorithms.

segments connecting the four realizable points can be pseudorandom encoded *using binary distributions*. However, other random distributions can be used to encode the entire region surrounded by curve $\mathbf{a}_8, \mathbf{a}_9, \mathbf{a}_{10}, \mathbf{a}_{11}, \mathbf{a}_8$. One approach for doing this is to build up more involved distributions out of combinations of binary distributions. The dashed line in Fig. 7 represents the set of values that could be encoded between $\mathbf{a}_9$ and $\mathbf{a}_c$ if the value $\mathbf{a}_c$ were part of the modulation characteristic. However the value $\mathbf{a}_c$ is the result of binary pseudorandom encoding using the values $\mathbf{a}_8$ and $\mathbf{a}_9$, and it is not part of the characteristic. Nonetheless it is possible to randomly select between $\mathbf{a}_9$ and $\mathbf{a}_c$ so that the desired value $\mathbf{a}_c'$ can be realized on average. This two step encoding formula was evaluated as being equivalent to a single encoding formula using a ternary distribution that selects between the points $\mathbf{a}_8$, $\mathbf{a}_9$, and $\mathbf{a}_{10}$. A derivation of such a formula (though not applied to discrete SLMs) is given in Ref. 31. From this analysis, it becomes apparent that by varying the value of $\mathbf{a}_c$ it is possible to encode the entire region interior to $\mathbf{a}_8, \mathbf{a}_9, \mathbf{a}_{10}, \mathbf{a}_8$ using a ternary encoding formula. The region interior to $\mathbf{a}_8, \mathbf{a}_{10}, \mathbf{a}_{11}, \mathbf{a}_8$ can be pseudorandom encoded in a similar manner.

4 Summary and Conclusions

The use of binary statistics leads to extremely simple pseudorandom encoding formulas. Perhaps the greatest value of using the binary distribution is that it provides significant insight and even a graphical interpretation of the operation and performance of pseudorandom encoding. Evaluations have been presented for a variety of amplitude-phase coupled SLM characteristics. In each case a convex region was identified by simple graphical constructions. An extremely simple formula for determining the encoding error was presented. Applying it to circular SLM characteristics showed there to be no advantage as to which pair of modulation values are used in the encoding formula. For noncircular SLM characteristics, however, significant reductions in encoding error are possible. We also found that phase-only SLMs that produce phase modulations greater than π but less than 2π can also be pseudorandomly encoded with fully complex functions. Also discussed were ways to build up more complicated functions out of combinations of binary distributions. This was used to demonstrate that discrete modulation characteristics can represent fully complex functions over a continuous region in the complex plane. This result is especially significant in light of the digital addressing of SLMs and the small number of phase steps used in most multilevel binary diffractive optics. Therefore, this analysis method proves to be a useful tool that can accelerate the development and broaden the applicability of pseudorandom encoding algorithms to a wide variety of amplitude-phase coupled modulator characteristics.

Acknowledgments

This study was supported by the National Aeronautics and Space Administration (NASA) cooperative agreement No. NCC5-222 and Office of Naval Research (ONR) grant No. N00014-96-1-1296.

References

1. B. R. Brown and A. W. Lohmann, ''Complex spatial filter,'' *Appl. Opt.* **5**, 967–969 (1966).
2. B. R. Brown and A. W. Lohmann, ''Computer-generated binary holograms,'' *IBM J. Res. Dev.* **13**, 160–168 (1969).
3. W. J. Dallas, ''Computer-generated holograms,'' Chap. 6 in *The Computer in Optical Research*, B. R. Frieden, Ed., pp. 291–366, Springer, Berlin (1980).
4. O. Bryngdahl and F. Wyrowski, ''Digital holography—computer-generated holograms,'' in *Progress in Optics XXVIII*, E. Wolf, Ed., pp. 1–86, Elsevier, Amsterdam (1990).
5. R. W. Cohn and L. G. Hassebrook, ''Representations of fully complex functions on real-time spatial light modulators,'' Chap. 15, in *Optical Information Processing*, F. T. S. Yu and S. Jutamulia, Eds., pp. 396–432, Cambridge University Press, Cambridge (1998).
6. R. W. Cohn, ''Real-time multispot beam steering with electrically controlled spatial light modulators,'' in *Optical Scanning Systems: Design and Applications*, L. Beiser and S. F. Sagan, Eds., *Proc. SPIE* **3131**, 145–155 (July 1997).
7. V. Kettunen, P. Vahimaa, and J. Turunen, ''Zeroth-order coding of complex amplitude in two dimensions,'' *J. Opt. Soc. Am. A* **14**(4), 808–815 (1997).
8. J. M. Florence and R. D. Juday, ''Full complex spatial filtering with a phase mostly DMD,'' *Proc. SPIE* **1558**, 487–498 (1991).
9. R. D. Juday and J. M. Florence, ''Full complex modulation with two one-parameter SLMs,'' *Proc. SPIE* **1558**, 499–504 (1991).
10. D. A. Gregory, J. C. Kirsch and E. C. Tam, ''Full complex modulation using liquid-crystal televisions,'' *Appl. Opt.* **31**(2), 163–165 (1992).
11. L. G. Neto, D. Roberge and Y. Sheng, ''Full-range, continuous, complex modulation by the use of two coupled-mode liquid-crystal televisions,'' *Appl. Opt.* **35**(23), 4567–4576 (1996).
12. L. B. Lesem, P. M. Hirsch and J. A. Jordon, Jr., ''The kinoform: a new wavefront reconstruction device,'' *IBM J. Res. Dev.* **13**, 150–155 (1969).
13. R. W. Gerchberg and W. O. Saxton, ''Practical algorithm for the determination of phase from image and diffraction plane pictures,'' *Optik (Stuttgart)* **35**(2), 237–250 (1972).
14. N. C. Gallagher and B. Liu, ''Method for computing kinoforms that reduces image reconstruction error,'' *Appl. Opt.* **12**(10), 2328–2335 (1973).
15. H. Stark, W. C. Catino, and J. L. LoCicero, ''Optical phase-mask design using generalized projections,'' *J. Opt. Soc. Am. A* **8**(3), 566–571 (Mar. 1991).
16. M. P. Dames, R. J. Dowling, P. McKee, and D. Wood, ''Efficient optical elements to generate intensity weighted spot arrays: design and fabrication,'' *Appl. Opt.* **30**(19), 2685–2691 (1991).
17. E. G. Johnson, M. A. Abushagur, ''Microgenetic-algorithm optimization methods applied to dielectric gratings,'' *J. Opt. Soc. Am. A* **12**(5), 1152–1160 (1995).
18. J. N. Mait, ''Understanding diffractive optic design in the scalar domain,'' *J. Opt. Soc. Am. A* **12**(10), 2145–2158 (1995).
19. R. D. Juday, ''Optimal realizable filters and the minimum Euclidean distance principle,'' *Appl. Opt.* **32**(26), 5100–5111 (1993).
20. R. D. Juday and J. Knopp, ''HOLOMED—an algorithm for computer generated holograms,'' *Proc. SPIE* **2752**, 162–172 (1996).
21. M. W. Farn and J. W. Goodman, ''Optimal maximum correlation filter for arbitrarily constrained devices,'' *Appl. Opt.* **28**(15), 3362–3366 (1989).
22. R. D. Juday, ''Correlation with a spatial light modulator having phase

and amplitude cross coupling,'' *Appl. Opt.* **28**(22), 4865–4869 (1989).
23. K. Lu and B. E. A. Saleh, ''Theory and design of the liquid crystal TV as an optical spatial phase modulator,'' *Opt. Eng.* **29**(3), 241–246 (1990).
24. C. Zeile and E. Luder, ''Complex transmission of liquid crystal spatial light modulators in optical signal processing applications,'' *Proc. SPIE* **1911**, 195–206 (1993).
25. J. L. Pezzaniti and R. A. Chipman, ''Phase-only modulation of twisted nematic liquid-crystal TV by use of the eigenpolarization states,'' *Opt. Lett.* **18**(18), 1567–1569 (1993).
26. C. Soutar, S. E. Monroe, Jr., and J. Knopp, ''Measurement of the complex transmittance of the Epson liquid crystal television,'' *Opt. Eng.* **33**(4), 1061–1068 (1994).
27. R. W. Cohn and M. Liang, ''Pseudorandom phase-only encoding of real-time spatial light modulators,'' *Appl. Opt.* **35**(14), 2488–2498 (1996).
28. R. Hauck and O. Bryngdahl, ''Computer-generated holograms with pulse-density modulation,'' *J. Opt. Soc. Am. A* **1**(1), 5–10 (1984).
29. R. W. Cohn and W. Liu, ''Pseudorandom encoding of fully complex modulation to bi-amplitude phase modulators,'' *Optical Society of America Topical Meeting on Diffractive Optics and Micro Optics*, 1996 OSA Technical Digest Series, Vol. 5, pp. 237–240, Boston, MA (1996).
30. R. W. Cohn, A. A. Vasiliev, W. Liu and D. L. Hill, ''Fully complex diffractive optics via patterned diffuser arrays,'' *J. Opt. Soc. Am. A* **14**(5), 1110–1123 (1997).
31. R. W. Cohn, ''Pseudorandom encoding of fully complex functions onto amplitude coupled phase modulators,'' *J. Opt. Soc. Am. A* **15**(4), 868–883 (1998).

Robert W. Cohn is a professor of electrical engineering and director of the ElectroOptics Research Institute at the University of Louisville. He holds his PhD degree from Southern Methodist University and his MS and BS degrees from the University of Kansas, Lawrence, all in electrical engineering. Prior to joining the university, from 1978 to 1989 Cohn was a member of the technical staff of Texas Instruments in Dallas, performing research on spatial light modulators for optical information processing, surface acoustic wave devices and microwave hybrid circuits for electronic signal processing, and tracking algorithms for imaging IR missile seekers. At the University of Louisville he continues research on the application and characterization of spatial light modulators as well as related work on the design, fabrication and measurement of diffractive optics. He is a member of SPIE and OSA and a senior member of IEEE.